Floresta Ambient., Rio de Janeiro, 2026; 33: e20250006
https://doi.org/10.1590/2179-8087-FLORAM-2025-0006
ISSN 2179-8087 (online)

ORIGINAL ARTICLE – Forest Products Science and Technology

Ionothermal Liquefaction of Mangrove Cellulose by Deep Eutectic Solvent Under Ambient Pressure

Ying Ki Ng[1]
Eric Wei Chiang Chan[2]
Muhammad Zhafran Zakaria[3]
Vannajan Sanghiran Lee[3]
Chen Wai Wong[4]

[1]UCSI University (UCSI), Faculty of Applied Sciences, Department of Food Science and Nutrition, Kuala Lumpur, Malaysia.

[2]UCSI University (UCSI), International Institute of Science Diplomacy and Sustainability, Kuala Lumpur, Malaysia.

[3]Universiti Malaya (UM), Faculty of Science, Department of Chemistry, Center of Excellence in Quantum Information Science and Technology, Kuala Lumpur, Malaysia.

[4]UCSI University (UCSI), Faculty of Applied Sciences, Department of Biotechnology, Kuala Lumpur, Malaysia.

Abstract

This study explores ionothermal liquefaction (ITL) of mangrove cellulose into levulinic acid (LA) using deep eutectic solvents (DES) under ambient pressure. Choline chloride-lactic acid (ChCl:Lac) and its $FeCl_3$-modified variant (DES-$FeCl_3$) were tested for cellulose breakdown and LA production. The highest yields (158.8 and 153.0 g/kg of delignified wood) were achieved with 1:7 DES at 180°C and 1:10 DES at 200°C. GC-MS and NMR confirmed LA as a major bio-oil component. Molecular dynamics simulations showed DES promotes cellulose depolymerization through hydrogen bonding, facilitating dehydration to LA. This approach offers an effective, low-impact alternative to acid hydrolysis, requiring no high-pressure systems or hazardous reagents. It demonstrates the potential for sustainable biofuel production in decentralized settings, reducing energy needs, minimizing environmental risks, and enhancing scalability, making it a promising pathway for eco-friendly biofuel technologies.

Keywords: Ionothermal liquefaction, Deep eutectic solvents, Levulinic acid, Green solvents, Mangrove biomass, Biofuels.

Key message

This study addresses the energy limitations of rural communities that depend heavily on charcoal for heating and energy. Advanced energy carriers like hydrogen and ammonia are not practical for these regions due to economic and infrastructural constraints. We present a practical solution by converting lignocellulosic biomass into levulinic acid (LA), a platform chemical with biofuel applications, through a cost-effective and scalable process. The method utilizes food-safe deep eutectic solvents (DES) and operates at relatively low temperatures (<200°C), significantly reducing energy requirements. This combination of low-temperature operation, safer solvents, and simplified apparatus offers a novel and viable pathway for sustainable energy production.

1. INTRODUCTION

Carbon dioxide emissions from fossil fuel combustion drive climate change, highlighting the need for sustainable energy, as emphasized in the Paris Agreement [Rashidi et al. 2022]. International agreements like the Ramsar Convention, REDD+, and CBD stress sustainable biomass use for energy and conservation [Harris et al., 2020; Berning & Sotirov, 2023].

Traditional biofuel production methods, including pyrolysis and hydrothermal liquefaction (HTL), rely on high temperatures, pressurised reactors, and corrosive acids, making them costly, hazardous, and environmentally unsustainable. These processes require complex auxiliary systems and corrosion-resistant infrastructure, further increasing engineering and operational costs. The conversion of lignocellulosic biomass to levulinic acid (LA), a key biofuel precursor, commonly involves harsh mineral acids such as sulphuric and hydrochloric acid, which present additional environmental and handling risks [Panisko et al., 2015; Bazoti et al., 2023]. Heterogeneous catalysts have emerged as a safer alternative, reducing acid use while achieving high LA yields. However, they still operate under high temperature and pressure, and their gradual deactivation necessitates costly

regeneration. These limitations highlight the need for simpler, safer, and more economical biomass conversion pathways.

Ionothermal liquefaction (ITL) using deep eutectic solvents (DES) offers a promising alternative to conventional biofuel production [Harris et al., 2020; Amoroso et al., 2021; Fanali et al., 2021; Huo et al., 2023]. Composed of bio-based hydrogen bond donors (HBD) and acceptors (HBA), DESs exhibit low vapor pressure, low toxicity, and high boiling points, enabling operation at ambient pressure. This eliminates the need for high-pressure infrastructure, simplifying biofuel production while reducing energy demands [Abbott et al., 2003; Abbott et al., 2004; Abbott et al., 2007; Singh et al., 2015; Ng et al., 2022]. Additionally, DES-based ITL avoids the use of corrosive mineral acid catalysts [Kang et al., 2018; Signoretto et al., 2019; Liu et al., 2020; Świątek et al., 2020; Wang et al., 2020; Berning & Sotirov, 2023], which are not only environmentally hazardous but also highly corrosive, necessitating specialized 904L corrosion-resistant steel that does not fully mitigate the risks of acid fuming [Lim et al., 2024]. By minimizing equipment wear and environmental risks, this approach enhances both process safety and sustainability while facilitating easier management and disposal of reactants [Toor et al, 2011; Wang et al, 2014].

This study investigates ambient pressure ITL of mangrove-derived cellulose into LA using DES system of choline chloride (ChCl) and lactic acid (Lac). Lac functions as both a Brønsted acid and HBD, while iron (III) chloride ($FeCl_3$) acts as a Lewis acid catalyst to enhance conversion efficiency. Operating at low temperatures (<200°C) and ambient pressure reduces energy demand, minimises hazardous substances, and increases process flexibility for decentralised applications [Kariim et al., 2023]. For the first time, this study demonstrates that ITL of lignocellulosic biomass can be conducted entirely in standard glass reactors using DESs, eliminating the need for high-pressure systems and corrosion-resistant infrastructure. This simplifies biomass conversion and enables practical, scalable biofuel production in rural, forest-dependent, and off-grid communities, particularly those rich in mangrove and other lignocellulosic resources. These findings support Sustainable Development Goals and international policies promoting low-impact biomass utilisation [Stevenson et al., 1999; Romañach et al., 2018].

2. MATERIALS AND METHODS

2.1. Raw material and delignification

Mangrove wood chips were sourced from Kamal Herba, a licensed supplier based in Kampung Dew, Semanggol, Malaysia. The biomass originated from the Matang Mangrove Forest Reserve in Perak, Malaysia, a 40,000 ha managed silviculture area dominated by *Rhizophora apiculata*. The area has been sustainably managed for mangrove timber and charcoal production since 1902.

The wood chips were delignified using a DES-assisted method. A total of 0.5 g of wood chips was mixed with 5 mL of ChCl:Lac DES (1:2 molar ratio) and heated at 60°C in a water bath for 3 hours. The wood chips were rinsed with methanol and oven-dried at 60°C for 1 hour. Lignin extraction was performed by adding 5 mL of butanol to the recovered DES, followed by vigorous mixing and phase separation using a separatory funnel. The organic layer was collected, and solvents were removed using a rotary evaporator. The efficiency of delignification was assessed indirectly using the Folin–Ciocalteu assay, with total phenolic content (TPC), expressed as gallic acid equivalents (g GAE/kg wood), serving as an indicator of lignin removal, though it also includes other wood extractives. Gallic acid, a common phenolic acid released during lignin breakdown.

2.2. Preparation of DES

ChCl-Lac DES was prepared by mixing ChCl and Lac at molar ratios of 1:2, 1:5, 1:7, 1:9, and 1:10, followed by heating in a 60°C water bath for one hour to aid dissolution [15]. The mixtures were cooled to room temperature while stirring, forming a homogeneous liquid, then dried using a rotary evaporator to remove excess water. The process was repeated for ChCl-Lac DES with $FeCl_3$ at ratios of 1:2:0.1, 1:5:0.1, 1:7:0.1, 1:9:0.1, and 1:10:0.1.

2.3. Ionothermal liquefaction

ITL of delignified mangrove wood was performed using a ChCl-Lac DES system, with and without the addition of $FeCl_3$ as a Lewis acid catalyst. For each experiment, 0.5 g of delignified wood chips was mixed with 5 mL of DES in a ceramic crucible and stirred evenly. The crucibles were heated in a muffle furnace (Ht40A PID controller) under the following conditions:

DES Ratios Tested: 1:2, 1:5, 1:7, 1:9, 1:10
Reaction Temperatures: 120°C, 140°C, 160°C, 180°C, 200°C

Each reaction was conducted for 2 hours, after which the crucibles were allowed to cool. Product extraction carried out by mixing 20 mL of distilled water and 10 ml butanol for phase extraction. The aqueous bottom layer was eluted, and the organic top layer was collected and concentrated by rotary evaporation at 80°C to remove butanol. To determine wood residue weight, the recovered solid residues were rinsed with methanol to remove excess DES and dried before weighing. The above procedure was repeated with

DES modified by $FeCl_3$ for all five ChCl-Lac ratios across the same range of reaction temperatures.

2.4. GC-MS identification of Bio-oil components

Bio-oil extracts were analyzed using GC-MS on a Shimadzu GC/MS QP2010 Ultra system (Shimadzu Co., Kyoto, Japan). Samples were diluted with 10 mL MeOH and injected (1 µL, 250°C, split ratio 10) into a 30 m, 0.25 mm ID SLB-5ms column (0.25 µm film thickness). Helium was used as the carrier gas (37.1 kPa, 0.8 mL/min). The GC temperature was programmed from 50 to 300°C (3°C/min) and held at 300°C for 10 min. Full-scan mass spectra (40–700 m/z) were collected with an MS transfer line at 250°C and an ion source at 200°C. Compounds were identified by comparing mass spectra with the NIST library database, reporting retention time, peak area (%), molecular formula, and molecular weight.

2.5. GC-FID quantification of levulinic acid

Diluted bio-oil extracts were analysed using an Agilent 7890A gas chromatograph equipped with a flame ionisation detector (GC-FID). Separation was performed on an Agilent HP-5 column (30 m × 0.32 mm ID × 3.5 µm film thickness; Agilent Technologies, USA). Helium was used as the carrier gas at a flow rate of 5 mL/min under a pressure of 18.654 psi, while hydrogen was used as the fuel gas for the detector at 30 mL/min. A 1 µL injection volume was employed at an injector temperature of 250°C with a split ratio of 1:10. The oven temperature was programmed from 60°C (held for 6 min) to 250°C at 10°C/min and held at 250°C for 10 min. The detector temperature was maintained at 250°C. A standard calibration curve for levulinic acid (LA) in the range of 1–16 mg/mL was constructed using the equation y = 505.19x, and LA content was expressed as g/kg of delignified wood.

Equation 1:
Given y = 505.19x, 10x dilution

$$\text{Yield of LA (g/kg of delignified wood)} = \frac{\text{Peak area}}{505.19} \times 10 \times 2$$

2.6. Isolation and purification of compounds

Bio-oil obtained from ITL using 1:10 DES at 140°C was purified via liquid column chromatography. The crude extract (10 g) was pre-absorbed onto silica gel (1:2), dried, and loaded into a silica gel 60 column (1:20). Elution used a chloroform:methanol:water gradient (9:1:0.1 to 6:4:1), with 20 mL fractions collected and analyzed by TLC, yielding five main fractions. Fractions 1, 3, and 4 underwent further purification.

Fraction 1 (0.46 g) was reprocessed using silica gel and eluted with chloroform:hexane (50:50 to 100%) and the same gradient. Fractions 3 and 4, processed using MCI gel and smaller-scale setups, were eluted with water:methanol (90:10 to 5:95) and 100% acetone. All purified extracts were dried and their yields recorded.

TLC used silica gel 60 F254 plates and various solvent systems. Developed plates were visualized under UV (254/365 nm) and post-treated with 0.05N H_2SO_4. Fractions with similar TLC profiles were pooled for final purification.

2.7. Nuclear magnetic resonance

Pure compounds from column chromatography were identified using NMR spectroscopy. Samples were dissolved in deuterated chloroform ($CDCl_3$) and methanol (CD_3OD) according to the solubility, and analyzed using a Bruker DRX-600 spectrometer (600 MHz for ^1H, 150 MHz for ^{13}C). Chemical shifts (δ) were recorded in ppm, and J-coupling values were measured from peak distances. Spectra were compared with literature values for compound identification.

2.8. Molecular dynamics simulations

The structures of Cellulotriose, ChCl, Lac, and water were obtained from PubChem and optimized using Density Functional Theory (DFT) with the B3LYP functional and 6-31G(d,p) basis set in Gaussian09. Geometry optimizations were performed to determine stable structures before molecular packing.

Molecular dynamics (MD) simulations were conducted using GROMACS 2024.1 with Packmol for initial structure construction. Monomers were placed in a low-density box and compressed until no further reduction was possible. The Charmm36 force field described solute-solvent interactions. Energy minimization was performed for 50,000 steps at 298.15 K and 1 bar, followed by gradual heating to 303.15 K.

After reaching equilibrium, a 3 ns NVT simulation was conducted with constraints applied via the LINCS algorithm and a 1.2 nm vdW cut-off. The particle mesh Ewald (PME) method handled long-range interactions. Finally, the system was equilibrated in an NPT ensemble for 30 ns under isothermal and pressure-controlled conditions.

2.9. Statistical analysis

All experiments were performed in triplicate (n = 3) and reported as mean ± SD. Data analysis was conducted using IBM SPSS Statistics 22. ANOVA was performed with

the Tukey HSD test for significance ($p < 0.05$). Correlations between variables were assessed using Pearson's correlation.

3. RESULTS AND DISCUSSION

3.1. Delignification and cellulose content

Effective delignification is essential to isolate cellulose for subsequent liquefaction. In this study, delignification efficiency was assessed indirectly by measuring the TPC extracted from the biomass, expressed as GAE. The conventional NaOH-based method removed 102.34 g GAE/kg wood, while DES-based delignification achieved 1,065.66 g GAE/kg wood, indicating substantially higher lignin removal. These results align with previous studies reporting the ability of ChCl-based DES to solubilise lignin and disrupt lignocellulosic structure [Liu et al., 2020].

After DES delignification and butanol extraction of remaining soluble fractions, the residual biomass primarily consisted of cellulose. Therefore, the subsequent ITL process targeted this cellulose fraction for conversion to LA. The observed reduction in solid residue mass and the confirmed production of LA by GC-MS, NMR, and GC-FID analyses collectively indicate successful cellulose breakdown.

3.2. Production of bio-oil by acid hydrolysis and solid catalysts

3.2.1. Loss of wood residue

ITL experiments with DES and DES-$FeCl_3$ produced finer wood particles than traditional acid hydrolysis (Table 1). Wood residue loss was calculated based on the initial and final weight of mangrove wood chips (w/w). The 1:5 and 1:9 DES mixtures at 200°C removed the most cellulose, leaving residue weights of 61.77% and 61.59%, respectively. This yield surpasses that of Li et al. (2013), who reported ~50% liquefaction at 210°C for 120 min with 0.01 mol/L sulfuric acid.

Table 1. Loss of wood residue (%) of biomass liquefaction by DES and DES-$FeCl_3$.

Solvent	Ratio	120°C	140°C	160°C	180°C	200°C
ChCl: Lac	1:2	32.95 ± 5.84^{bA}	48.50 ± 10.56^{abAB}	51.45 ± 5.03^{abA}	56.75 ± 3.06^{aA}	55.54 ± 8.23^{abB}
	1:5	37.42 ± 13.08^{aA}	56.71 ± 9.04^{aA}	39.01 ± 5.07^{aAB}	44.91 ± 8.55^{aABC}	61.77 ± 0.78^{aA}
	1:7	23.43 ± 20.27^{aA}	48.65 ± 6.35^{aAB}	42.85 ± 6.98^{aAB}	58.37 ± 6.44^{aA}	50.87 ± 19.20^{aABC}
	1:9	38.82 ± 2.52^{aA}	49.62 ± 7.78^{aAB}	37.31 ± 14.63^{aAB}	53.14 ± 5.31^{aA}	61.59 ± 1.74^{aA}
	1:10	34.20 ± 1.49^{cA}	24.72 ± 2.23^{cdB}	18.90 ± 2.88^{dB}	47.02 ± 5.87^{bAB}	59.20 ± 0.71^{aB}
ChCl: Lac: $FeCl_3$	1:2:0.1	37.49 ± 8.39^{aA}	68.01 ± 8.57^{aA}	28.31 ± 15.59^{aAB}	34.85 ± 13.16^{aABCD}	38.79 ± 14.64^{aABCD}
	1:5:0.1	33.14 ± 7.37^{bA}	51.93 ± 3.48^{aA}	30.37 ± 2.87^{cAB}	13.39 ± 4.79^{dD}	11.28 ± 4.52^{dD}
	1:7:0.1	22.79 ± 2.40^{bcA}	55.08 ± 4.62^{aA}	43.37 ± 6.92^{abAB}	15.60 ± 9.69^{cCD}	21.65 ± 11.06^{bcBCD}
	1:9:0.1	31.40 ± 7.13^{aA}	55.35 ± 10.48^{aA}	23.65 ± 23.30^{aAB}	14.56 ± 15.32^{aD}	21.83 ± 16.46^{aBCD}
	1:10:0.1	40.68 ± 2.87^{aA}	48.91 ± 4.82^{aAB}	36.21 ± 3.66^{abAB}	21.09 ± 2.10^{bcBCD}	15.38 ± 10.44^{cCD}

[a] Data are reported as mean ± SD (n=3) with different superscripts (a-d) indicate significant differences from each other ($p<0.05$) within the same row, superscripts (A-D) indicate significant differences from each other ($p<0.05$) within the same column.

[b] % are calculated based by weight of weight residue and weight of initial mangrove wood chips (w/w).

The improved efficiency of DES-based ITL in reducing wood residue and producing finer particles is attributed to cellulose's solubility and reactivity in DES. Zhang et al. (2020) reported that ChCl-based DES forms hydrogen bonds with cellulose hydroxyls and amino groups, enhancing dissolution. At higher temperatures, increased cellulose solubility and reduced DES viscosity improve mass transfer and cellulose interaction [Zhang et al, 2020].

$FeCl_3$ was investigated due to its role as a Lewis acid catalyst in oxidation, esterification, and condensation reactions. However, DES-$FeCl_3$ reactions resulted in less wood residue loss than DES alone. Prior studies using Ni^{2+} and Fe^{3+} as co-catalysts in non-aqueous solvents showed only marginal improvements over protic solvents. This suggests that while Fe^{3+} enhances hydrolysis in aqueous systems, its effectiveness is limited in non-aqueous DES due to lower water availability [Chen et al., 2016; De Caprariis et al., 2021].

These findings align with Hurst et al. (2019), who observed variable solid yields (38-63 wt%) from poplar wood after acid catalysis at 160-200°C using a microwave reactor. The comparison underscores ITL's potential as an effective low-temperature, low-pressure alternative for cellulose dissolution using ChCl-Lac DES, offering a sustainable biomass conversion approach.

3.2.2. GC-MS identification of bio-oil components

Figure 1 shows 1:10 DES and 1:10:0.1 DES-$FeCl_3$ at 140°C. LA was detected at a retention time of 17.320 with a peak area of 66.32%, along with methyl ester LA (32.05%) and dipentyl ketone (1.63%). Further analysis revealed LA at retention times of 16.010 and 15.593 with peak areas of 2.05% and 2.80%, respectively. Other value-added products such as γ-butyrolactone and lactic acid (Lac) were identified, though Lac is likely extracted from DES during partitioning. Full GC-MS compound identifications are shown in Table 2.

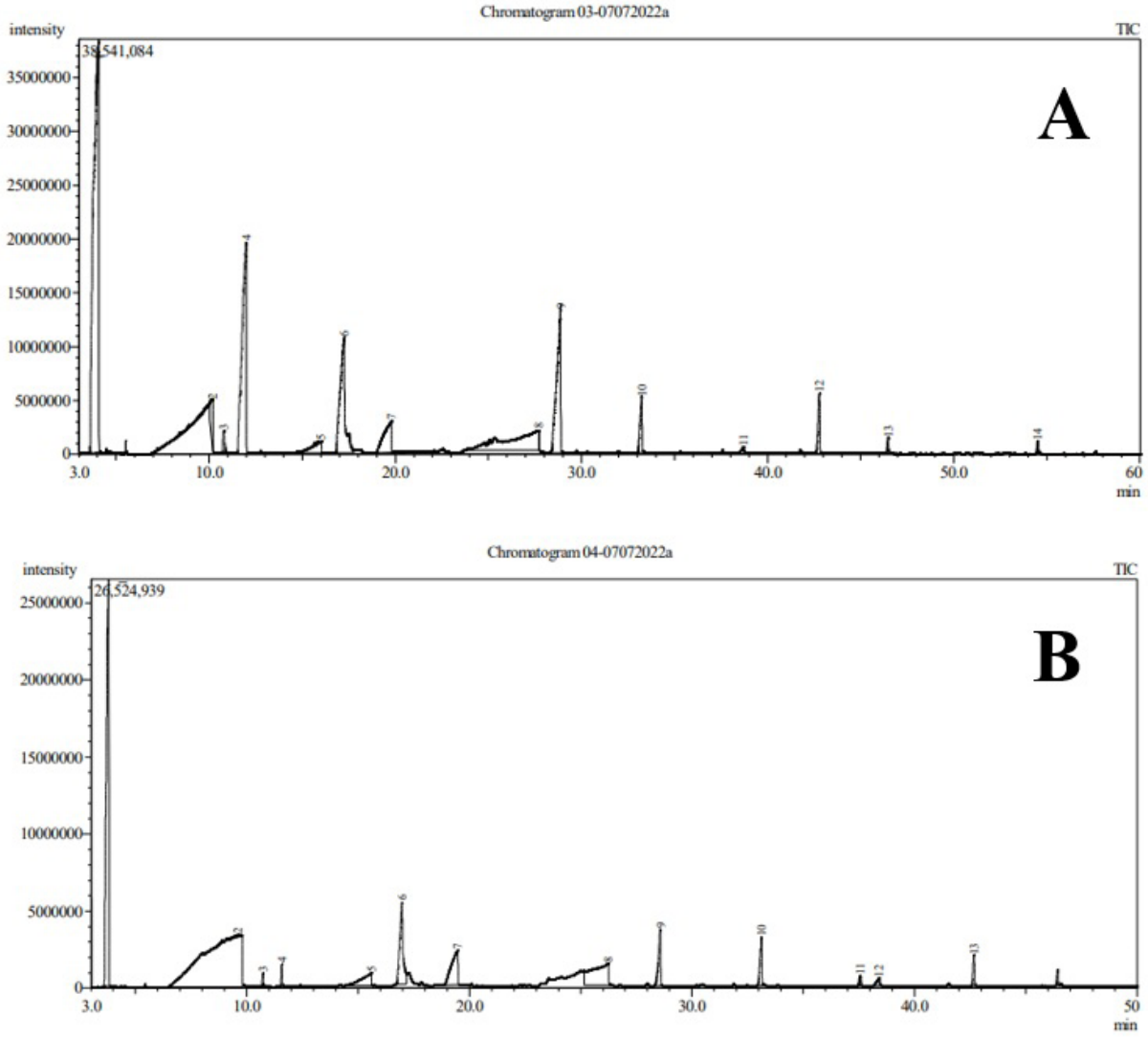

Figure 1. GC-MS chromatograms of (A)1:10 DES (B)1:10:0.1 DES-$FeCl_3$.

Table 2. Identification of compounds from acid hydrolysis and ionothermal liquefaction of mangrove cellulose at 140ºC.

Sample	No.	Retention time	Compound	Compound ID	Chemical formula	CAS	Molecular weight	Peak Area (%)
LA standard	1	10.537	Methyl ester levulinic acid	11579	$C_6H_{10}O_3$	624-45-3	130	1.63
	2	12.595	Dipentyl ketone	13561	$C_{11}H_{22}O$	927-49-1	170	32.05
	3	17.320	Levulinic acid	11579	$C_5H_8O_3$	123-76-2	116	66.32
1M H_2SO_4+Al_2O_3	1	10.863	Methyl ester levulinic acid	11579	$C_6H_{10}O_3$	624-45-3	130	98.69
	2	18.349	Pentanoic acid, 4,4-dimethoxy-, ethyl ester	71309430	$C_9H_{18}O_4$	109-52-4	190	1.31
1:10 DES	1	4.053	γ-butyrolactone	123740	$C_4H_2D_4O_2$	65364-43-4	86	38.57
	2	10.180	Lactic acid	612	$C_3H_6O_3$	79-33-4	90	1.72
	3	10.778	Methyl ester levulinic acid	11579	$C_6H_{10}O_3$	624-45-3	130	0.61
	4	11.985	Butyl lactate	91435	$C_7H_{14}O_3$	138-22-7	146	16.00
	5	16.010	Levulinic acid	11579	$C_5H_8O_3$	123-76-2	116	2.05
	6	17.241	Propanoic acid, 2-(methoxymethoxy)	1032	$C_5H_{10}O_5$	81327-29-9	134	10.44
	7	19.776	2,4-Pentanediol	12262	$C_6H_{14}O_2$	5683-44-3	118	4.40
	8	27.686	Propanoic acid	1032	$C_{12}H_{24}O_3$	74367-31-0	216	10.68
	9	28.862	Butyl ester lactic acid	518439	$C_7H_{14}O_3$	138-22-7	146	10.27
	10	33.237	Formic acid	284	$C_5H_{10}O_2$	589-40-2	102	2.25
	11	38.699	Propanoic acid, 2-hydroxy-, butyl ester	87794013	$C_7H_{14}O_3$	138-22-7	146	0.33
1:10:0.1 DES-$FeCl_3$	1	3.794	Ethyl alcohol	702	C_2H_6O	64-17-5	46	23.08
	2	9.596	Lactic acid	612	$C_3H_6O_3$	79-33-4	90	45.47
	3	10.710	Methyl ester levulinic acid	11579	$C_6H_{10}O_3$	624-45-3	130	0.30
	4	11.574	Butyl lactate	91435	$C_7H_{14}O_3$	138-22-7	146	0.58
	5	15.593	Levulinic acid	11579	$C_5H_8O_3$	123-76-2	116	2.80
	6	16.972	Propanoic acid, 2-(methoxymethoxy)	1032	$C_5H_{10}O_5$	81327-29-9	134	6.42
	7	19.463	2,4-Pentanediol	12262	$C_6H_{14}O_2$	5683-44-3	118	4.40
	8	26.243	Propanoic acid	1032	$C_{12}H_{24}O_3$	74367-31-0	216	8.39
	9	28.579	Butyl ester lactic acid	518439	$C_7H_{14}O_3$	138-22-7	146	3.09
	10	33.122	Formic acid	284	$C_5H_{10}O_2$	589-40-2	102	2.31
	11	37.541	Vanilic acid hydrazide	8468	$C_8H_{10}N_2O_3$	100377-63-7	182	0.38
	12	38.398	Propanoic acid, 2-hydroxy-, butyl ester	87794013	$C_7H_{14}O_3$	138-22-7	146	0.59
	13	42.679	Tetraethylene glycol	8200	$C_{12}H_{26}O_5$	1559-34-8	250	1.15

Renumbered figures, to avoid citing figures twice this sentence now direct reader to section

The major compounds in chromatogram A included ethyl alcohol (38.57%), lactic acid (1.72%), methyl ester LA (0.61%), butyl lactate (16%), LA (2.05%), propanoic acid (10.68%), butyl ester lactic acid (10.27%), formic acid (2.25%), and butyl ester propanoic acid (0.33%). In chromatogram B, the composition differed slightly, with ethyl alcohol (23.08%), lactic acid (45.47%), methyl ester LA (0.30%), butyl lactate (0.58%), LA (2.8%), propanoic acid (6.42%), butyl ester lactic acid (3.09%), formic acid (2.31%), vanillic acid hydrazide (0.38%), butyl ester propanoic acid (0.59%), and tetraethylene glycol (1.15%).

Study reported methyl levulinate formation from cellulose at higher temperatures, suggesting ITL can achieve similar yields under milder conditions [Zhou et al., 2019]. Methyl ester LA, consistently detected across samples, serves as a bio-based solvent but presents challenges as a biofuel precursor due to its high oxygen content and low energy density [Zhou et al., 2019]. However, studies suggest long-chain levulinate esters offer improved energy density and hydrophobicity, making them better suited for biofuel applications [Itabaiana Junior et al., 2020; Jia et al., 2020].

GC-MS identification paves the way for LA quantification, reinforcing its role as a versatile platform molecule for conversion into high-energy biofuels. The presence of LA and its methyl ester as major bio-oil components supports ITL as a viable alternative to high-pressure liquefaction.

3.2.3. GC-FID quantification of levulinic acid

Bio-oils from DES yielded high LA levels, particularly at higher temperatures and ratios, as quantified by GC-FID (Table 3). The highest yields were from 1:7 DES at 180°C (158.8 g/kg, 15.9%) and 1:10 DES at 200°C (153.0 g/kg, 15.3%), confirming ChCl:Lac DES efficiently liquefies cellulose into LA at ambient pressure.

The effectiveness of DES, especially those with strong Brønsted acids, in biomass fractionation and catalytic enhancement is notable. Higher temperatures and DES ratios improve dehydration reactions, promoting cellulose-to-LA conversion. Compared to previous studies such as Hurst et al. (2019) and Ma et al. (2021), which required high pressures and strong acids to achieve LA yields up to 21.0 wt% (sulfuric acid) and 59.24% (Amberlyst-15 under nitrogen), our study demonstrates DES achieves comparable yields at atmospheric pressure [Ma et al., 2010; Hurst et al., 2019].

These findings highlight DES as an energy-efficient, lower-impact alternative to conventional acid hydrolysis, offering similar LA production with reduced complexity and cost. The eutectic point at 1:7 ChCl:Lac and 180°C optimizes LA yield, reinforcing DES's potential for sustainable biofuel production.

Table 3. Yield of levulinic acid (g/kg of delignified wood) by ionothermal liquefaction.

Solvent	Ratio	120°C	140°C	160°C	180°C	200°C
ChCl: Lac	1:2	9.946 ± 0.72^{abBC}	2.337 ± 1.78^{bA}	39.74 ± 19.30^{aCDE}	35.56 ± 2.12^{aD}	39.18 ± 6.49^{aBC}
	1:5	30.89 ± 6.73^{bcAB}	11.71 ± 5.45^{cA}	89.25 ± 6.01^{abABC}	148.3 ± 20.77^{aAB}	121.6 ± 34.59^{aAB}
	1:7	43.55 ± 2.29^{cA}	41.75 ± 2.70^{cA}	110.3 ± 22.18^{abA}	158.8 ± 23.10^{aA}	74.39 ± 21.37^{bcABC}
	1:9	29.56 ± 3.38^{aAB}	70.36 ± 80.00^{aA}	90.56 ± 22.99^{aAB}	140.2 ± 30.65^{aAB}	148.8 ± 0.95^{aA}
	1:10	24.94 ± 17.91^{bcABC}	13.32 ± 7.13^{cA}	44.11 ± 6.33^{bcBCDE}	100.0 ± 23.87^{abBC}	153.0 ± 41.32^{aA}
ChCl: Lac: $FeCl_3$	1:2:0.1	5.543 ± 1.01^{aC}	6.383 ± 0.54^{aA}	8.451 ± 9.88^{aE}	4.229 ± 2.82^{aD}	2.421 ± 3.42^{aC}
	1:5:0.1	4.940 ± 4.08^{bC}	17.63 ± 8.66^{bA}	56.89 ± 9.63^{aBCDE}	12.33 ± 5.26^{bD}	1.696 ± 2.40^{bC}
	1:7:0.1	4.039 ± 2.86^{cC}	19.68 ± 5.78^{bcA}	86.06 ± 10.05^{aABCD}	42.65 ± 8.46^{bCD}	20.10 ± 9.62^{bcC}
	1:9:0.1	8.733 ± 2.22^{cBC}	57.44 ± 4.67^{abA}	75.76 ± 15.22^{aABCD}	34.05 ± 10.83^{bcD}	18.31 ± 15.26^{cC}
	1:10:0.1	2.421 ± 3.42^{bC}	65.32 ± 7.45^{abA}	37.92 ± 5.47^{bDE}	48.11 ± 6.43^{abCD}	128.5 ± 59.48^{aAB}

Data are reported as mean ± SD (n=3) with different superscripts (a-c) indicate significant differences from each other ($p<0.05$) within the same row, superscripts (A-E) indicate significant differences from each other ($p<0.05$) within the same column.

3.3. Structural elucidation of LA

Bio-oil (10 g) from mangrove biomass liquefied at 140°C underwent solvent partitioning, yielding five fractions, with Fraction 1 containing the highest LA content. This fraction was further purified using Silica gel 60 column chromatography, resulting in seven pooled fractions (1.1 to 1.7) based on TLC profiles. Fraction 1.5 had the highest LA purity (95.78%), amounting to 957.8 mg/g, making it suitable for NMR structural elucidation (Table 4).

Table 4. Compounds extracted from column chromatography and comparison of ^{1}H and ^{13}C NMR spectral data of compound 3 (LA) with previous study.

Extract	Column	Fraction	Dry mass (mg)	Yield (%)*	LA Content
Bio-oil from liquefaction of mangrove wood	Solvent Partitioning	1	458.7	4.59	
		2	181.9	1.82	
		3	262.1	2.62	
		4	995.3	9.95	
		5	98.6	0.99	
Fraction 1	Silica gel 60	1.1	4.8	1.05	957.8mg/g
		1.2	1.4	0.31	
		1.3	65.6	14.30	
		1.4	28.7	6.26	
		1.5	167.0	36.41	
		1.6	8.3	1.81	
		1.7	48.5	10.57	

*Yield expressed as % w/w of the extract/fraction before separation.

These results demonstrate that LA can be effectively isolated using simple solvent partitioning and silica gel chromatography. This method achieves high-purity LA, making it suitable as a platform chemical in pharmaceuticals and other industries. However, for biofuel applications, a simpler fractional distillation process may suffice, as higher purity is unnecessary.

The highest recovery yield was observed in Fraction 4 (10%), followed by Fraction 3 (4.6%) and Fraction 2 (2.6%). A hexane-methanol-water-chloroform solvent system was used to separate compounds based on polarity, with hexane extracting non-polar compounds, methanol extracting polar compounds, water increasing polarity, and chloroform decreasing it.

For Fractions 3 and 4, MCI gel was employed as a reversed-phase stationary phase due to its hydrophilic polystyrene-divinylbenzene resin composition. Acetone was used in the final elution to recover remaining compounds. Compounds were considered for NMR analysis if they met two criteria: a single TLC band and weight exceeding 20 mg. Seven compounds were analyzed by NMR.

The target compound, LA, was found in the second and third fractions of Fraction 1, with the third containing the highest purity LA (Table 4). However, other isolated compounds lacked sufficient purity for identification. Yield percentages were calculated as w/w ratios of fraction yield to initial bio-oil mass (10 g).

The presence of LA (compound 3) was confirmed by TLC and NMR spectroscopy. TLC analysis showed LA exhibited a characteristic curve under visible light, an Rf value of 0.48, and UV absorption at 254 nm but not at 365 nm. It appeared as a dark brown liquid, and NMR studies verified its structure.

In ^{1}H NMR analysis, a singlet at δ 2.22 ppm indicated a methyl group (-CH_3), while triplets at δ 2.65 and δ 2.77 ppm with a J value of 6 Hz corresponded to methylene (-CH_2) groups. The ^{13}C NMR spectrum confirmed two carbonyl groups (C=O) at δ 178.2 and 206.7 ppm, methylene groups at δ 27.7 and 37.7 ppm, and a methyl group at δ 29.8 ppm. These spectral values were consistent with previous studies, confirming LA's identity (Table 5).

Previous studies further validated these ^{1}H and ^{13}C NMR spectral data, confirming LA's identity in our samples. These findings are critical as they confirm successful isolation and identification of LA while also providing a bio-oil composition indicator based on weight—a direct approach contrasting with mass-to-charge (m/z) ratio-based GC-MS analysis [Son et al., 2012; Yue et al., 2018].

Table 5. Comparison of ^{1}H and ^{13}C NMR spectral data of levulinic acid (compound 3) isolated from mangrove-derived bio-oil with previously reported values.

Atom	δH[a]	δH[b]	δC[a]	δC[b]
1	2.22 (s)	2.12 (s)	29.8	29.0
2	-	-	206.7	212.5
3	2.65 (t, 6.0)	2.49 (t)	27.7	27.9
4	2.77 (t, 6.0)	2.79 (t)	37.7	37.7
5		-	178.2	176.9

[a] Present study; [b] literature values [34,35]; δ values for ^{1}H (600 MHz) and ^{13}C (150 MHz) are reported in ppm; coupling constants (J) are given in Hz; s = singlet; t = triplet.

3.4. Molecular dynamics simulations

The parameters of different DES systems are shown in Table 6, with ChCl:Lac ratios of 1:2, 1:5, 1:7, 1:9, and 1:10 (Systems A–E). These were compared with water-based systems (F–H) for cellulose hydrolysis. Acid hydrolysis, a classic method for breaking down cellulose into glucose, was contrasted with the role of DES in cellotriose dissolution. The study examined the structural, energetic, and dynamic properties of DES and its impact on cellulose dehydration and hydrolysis.

Table 6. Details on no of DES and Water in a simulation box.

System	Ratio	No of ChCl	No of Lac	No of water	Yield of levulinic acid (g/kg)
A	1:2	137	274	0	
B	1:5	137	685	0	
C	1:7	137	959	0	
D	1:9	137	1233	0	
E	1:10	137	1370	0	
F	Water	0	0	1400	
G	1:2+water	137	274	700	
H	1:9+Water	137	1233	700	

A= ChCl:Lac DES with ratio 1:2; B= ChCl:Lac DES with ratio 1:5; C= ChCl:Lac DES with ratio 1:7; D= ChCl:Lac DES with ratio 1:9; E= ChCl:Lac DES with ratio 1:10; F= Full water solvent; G= Half 1:2 ChCl:Lac DES with half water solvent; H= Half 1:9 ChCl:Lac DES with half water solvent.

MD simulations revealed that ionothermal liquefaction by ChCl:Lac DES proceeds via 5-HMF as a key intermediate, supporting findings which identified levoglucosan in pyrolysis and glucose in hydrolysis [Hurst et al., 2019; Wang et al., 2020]. DFT studies confirmed that dehydration occurs primarily at -O2H, -O3H, and -O6H hydroxyl groups, forming 5-HMF and levoglucosan, followed by 5-HMF rehydration to LA and formic acid. Radial distribution function (RDF) analyses showed that Lac interacts with cellotriose, catalyzing dehydration and increasing LA yield as Lac concentration rises.

Optimal interaction distances were noted at 5 Å for Lac at hydroxyl groups and 7–8 Å for ChCl. with Lac–H bond distances ranging from 2.4 to 2.6 Å. The solvation structure of cellotriose surrounded by Lac is shown in Figure 2, while the binding of water molecules to Lac and cellotriose is illustrated in Figure 3. The distances between Lac and hydroxyl groups (-O2H, -O3H, -O6H) measured 2.26, 2.46, and 2.66Å, respectively, confirming -O2H as the most effective binding site. Dehydration, a crucial step in cellulose conversion, facilitates keto-enol rearrangement, significantly lowering the reaction's potential barrier, as described by Zhang et al. (2016). The acidic sites of Lac reduce energy barriers, improving cellotriose conversion to HMF.

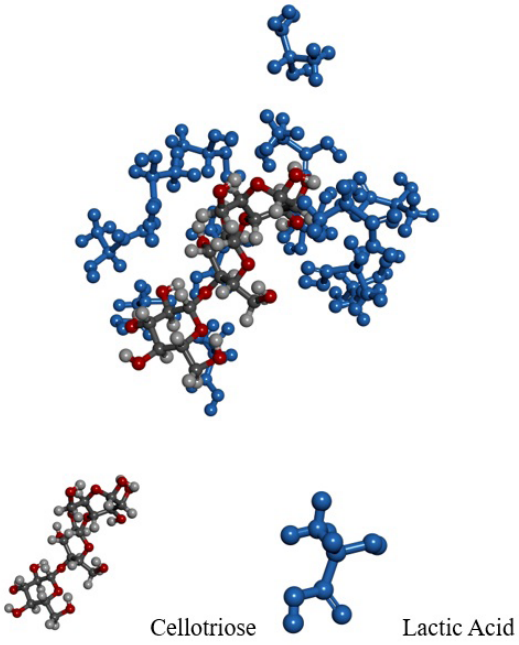

Figure 2. Solvation structure of cellotriose surrounded by Lac at 5Å.

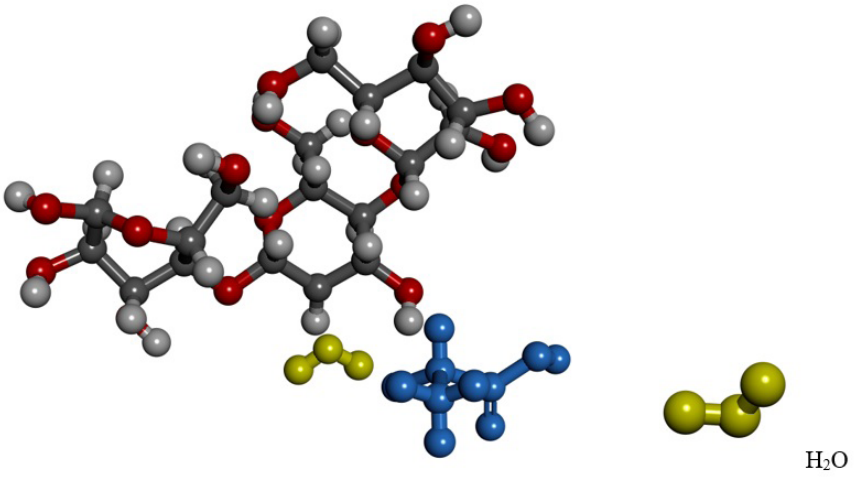

Figure 3. Binding of H_2O from cellotriose to Lac.

Lac was essential for DES performance, as systems without Lac showed lower LA yields despite greater thermal stability (Section 4.3.6). MD and DFT analyses confirmed that Lac binds hydroxyl groups more efficiently than ChCl (7–8Å), facilitating levoglucosan-to-5-HMF conversion. The non-aqueous nature of DES further enhances this process.

However, cellulose-to-levoglucosan conversion requires hydrolysis, which depends on water. In DES systems, water acts as a reactant rather than a solvent, originating from Lac's hygroscopic nature. Unless dehydrated with molecular sieves, Lac retains some water. In open systems, Lac absorbs atmospheric moisture, replenishing lost water in hydrolysis reactions, maintaining efficiency in LA production.

Water in DES systems appears to weaken dehydration potential, particularly when Lac is in excess.

Solvent Accessible Surface Area (SASA) analysis reveals key trends regarding DES behavior in water-free versus water-containing environments, as shown in Figure 4. Since SASA measures solvent-solute interactions, variations across different systems provide insight into DES as a dehydration agent, particularly in ITL at ambient pressure.

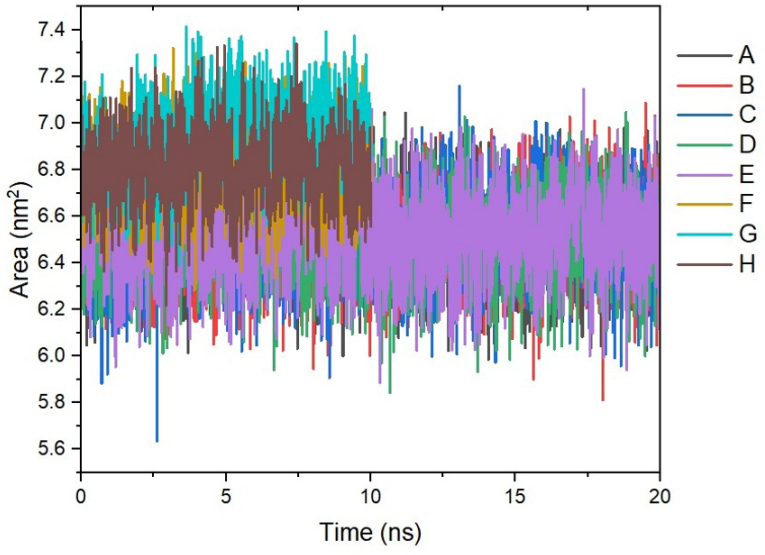

Figure 4. SASA of cellotriose in ChCl/Lac and ChCl/Lac + water systems over time (ns). Systems A–E are water-free, and F–H are water-containing, showing reduced SASA at higher Lac content and increased SASA in the presence of water.

In water-free systems (A–E), increasing Lac content leads to SASA reduction, indicating greater solute shielding. System E (1:10 ChCl) exhibits stable, low SASA (~6.4 nm²), while System A (1:2 ChCl) has slightly higher, more variable SASA (~6.8 nm²). At higher Lac concentrations, DES components form stronger hydrogen bonds, creating a compact structure with reduced solvent exposure, reinforcing dehydration efficiency.

In water-containing systems (G, H), SASA increases significantly. System H (1:9 ChCl + Water) shows the highest SASA (~7.4 nm²), while System G (1:2 ChCl + Water) is elevated (~7.0 nm²) compared to water-free DES systems. Pure water (System F) has a lower SASA (~6.0 nm²). This suggests that DES does not fully displace water from the solute surface but interacts dynamically with both water and solute, leading to partial hydration or solute-solvent exchange.

The elevated SASA in water-containing systems may seem counterintuitive for a dehydration agent, but it can be explained by DES-induced solute restructuring. Rather than compacting the solute, DES disrupts water-solute interactions, increasing solvent-exposed areas.

Comparing water-free (A–E) and water-containing (G, H) systems reveals that in the absence of water, DES reduces solvent-exposed areas, especially at higher Lac concentrations, confirming strong DES-solute interactions. When water is present, SASA increases, suggesting DES cannot fully exclude water from the solute surface. In System H, the high Lac ratio leads to the highest SASA (~7.4 nm²) due to excess Lac and water molecules.

The overall reaction pathway for the formation of levulinic acid and lactic acid from cellulose via ITL is illustrated in Figure 5. These results indicate that DES acts as an effective dehydration agent under water-free conditions, with higher Lac concentrations strengthening DES–solute interactions. However, in the presence of water, this efficiency is reduced, suggesting that solute–solvent interactions in such systems require further investigation.

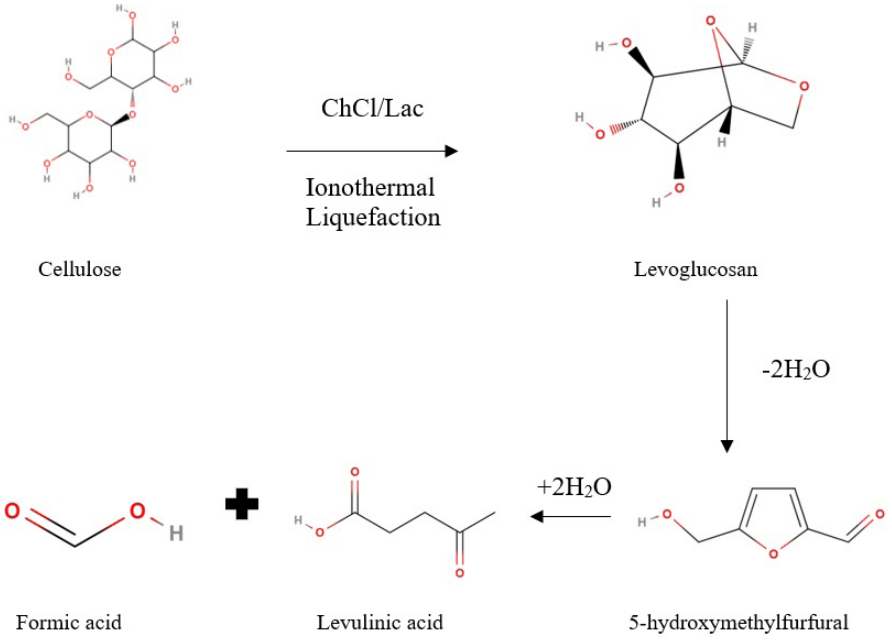

Figure 5. Proposed mechanism of formation of levulinic acid and lactic acid from ITL of cellulose by ChCl-Lac DES.

4. CONCLUSION

This study demonstrated the ITL of mangrove cellulose into LA using DES under ambient pressure. Optimized DES formulations, particularly 1:7 at 180°C and 1:10 at 200°C, achieved the highest LA yields. Chromatographic separation and NMR analysis confirmed the purity of LA, highlighting DES's efficiency in cellulose conversion without high-pressure reactors or corrosive acids. Molecular dynamics simulations revealed that lactic acid interacts with cellulose hydroxyl groups (-O2H, -O3H, -O6H), facilitating dehydration and forming levoglucosan and 5-HMF, which convert to LA. DES acts as a dehydration agent, reducing the energy barrier for cellulose breakdown. DES-based ITL offers a sustainable, cost-effective biofuel precursor production method, reducing energy use, environmental impact, and infrastructure costs. Future research should optimize solvent recyclability, minimize side products, and refine computational models to enhance catalyst interactions in DES systems, supporting broader adoption of sustainable biofuel technologies.

ACKNOWLEDGEMENTS

The authors gratefully acknowledge financial support from the Ministry of Higher Education (MOHE), Malaysia, under the Fundamental Research Grant Scheme (FRGS) (Grant No. FRGS/1/2022/STG04/UCSI/02/2).

SUBMISSION STATUS

Received: 01 Apr. 2025
Accepted: 24 Mar. 2026
Associate editor: Fernando Gomes

CORRESPONDENCE TO

Eric Wei Chiang Chan
Jalan UCSI, 1, Cheras 56000, Kuala Lumpur, Malaysia
e-mail: chanwc@ucsiuniversity.edu.my

AUTHORS' CONTRIBUTIONS

Ying Ki Ng: conceptualization (equal), data curation (lead), formal analysis (lead), investigation (equal), methodology (lead), project administration (lead), validation (equal), visualization (equal), writing – original draft (lead), writing – review & editing (lead).
Eric Wei Chiang Chan: conceptualization (equal), data curation (equal), funding acquisition (lead), methodology (lead), project administration (lead), resources (lead), supervision (lead), writing – review & editing (lead).
Muhammad Zhafran Zakaria: data curation (equal), investigation (equal), methodology (equal), project administration (equal), software (lead), validation (equal), visualization (equal), writing – original draft (equal).
Vannajan Sanghiran Lee: investigation (equal), methodology (equal), resources (equal), software (equal), supervision (equal), validation (equal).

Chen Wai Wong: conceptualization (equal), resources (equal), supervision (equal).

DATA AVAILABILITY

The datasets generated and analysed during this study are included in this published article and its supplementary materials. Additional data supporting the findings of this study are available from the corresponding author upon reasonable request.

REFERENCES

Rashidi NA, Chai YH, Yusup S. Biomass energy in Malaysia: current scenario, policies, and implementation challenges. Bioenergy Research 2022; 15:1371–1386.

Berning L, Sotirov M. Hardening corporate accountability in commodity supply chains under the European Union deforestation regulation. Regulation & Governance 2023; 17(4):870–890.

Harris S, Weinzettel J, Levin G. Implications of low carbon city sustainability strategies for 2050. Sustainability 2020; 12(13):5417.

Bazoti SF, Bonatto C, Scapini T, Camargo AF, Treichel H, De Oliveira D. Recent advances, perspectives and challenges on levulinic acid production from residual biomass. Biofuels Bioproducts Biorefining 2023; 17(4):1068–1084.

Panisko E, Wietsma T, Lemmon T, Albrecht K, Howe D. Characterization of the aqueous fractions from hydrotreatment and hydrothermal liquefaction of lignocellulosic feedstocks. Biomass Bioenergy 2015; 74:162–171.

Amoroso R, Hollmann F, Maccallini C. Choline chloride based DES as solvents, catalysts and chemical donors in pharmaceutical synthesis. Molecules 2021; 26:6286.

Fanali C, Gallo V, Della Posta S, Dugo L, Mazzeo L, Cocchi M, et al. Choline chloride–lactic acid-based NADES as an extraction medium in a response surface methodology-optimized method for the extraction of phenolic compounds from hazelnut skin. Molecules 2021; 26(9):2652.

Huo D, Sun Y, Yang Q, Zhang F, Fang G, Zhu H, et al. Selective degradation of hemicellulose and lignin for improving enzymolysis efficiency via pretreatment using deep eutectic solvents. Bioresource Technology 2023; 376:128937.

Abbott AP, Capper G, Davies DL, Rasheed RK, Tambyrajah V. Novel solvent properties of choline chloride/urea mixtures. Chemical Communications 2003; 1:70–71.

Abbott AP, Boothby D, Capper G, Davies DL, Rasheed RK. Deep eutectic solvents formed between choline chloride and carboxylic acids: versatile alternatives to ionic liquids. Journal of the American Chemical Society 2004; 126(29):9142–9147.

Abbott AP, Cullis PM, Gibson MJ, Harris RC, Raven E. Extraction of glycerol from biodiesel into a eutectic-based ionic liquid. Green Chemistry 2007; 9:868–872.

Ng YK, Lim WY, Lee VS, Lee KM, Wong CW, Chan EWC. Deep eutectic solvents as green and efficient media for biocatalytic processes. In: Current Developments in Biotechnology and Bioengineering. Elsevier; 2022. p. 161–180.

Singh R, Prakash A, Balagurumurthy B, Bhaskar T. Hydrothermal liquefaction of biomass. In: Recent Advances in Thermo-Chemical Conversion of Biomass. 2015. p. 269–291.

Kang S, Fu J, Zhang G. From lignocellulosic biomass to levulinic acid: a review on acid-catalyzed hydrolysis. Renewable and Sustainable Energy Reviews 2018; 94:340–362.

Liu Z, Hou Y, Hu S, Li Y. Possible dissolution mechanism of alkali lignin in lactic acid-choline chloride under mild conditions. RSC Advances 2020; 10(67):40649–40657.

Signoretto M, Taghavi S, Ghedini E, Menegazzo F. Catalytic production of levulinic acid from actual biomass. Molecules 2019; 24:2760.

Świątek K, Gaag S, Klier A, Kruse A, Sauer J, Steinbach D. Acid hydrolysis of lignocellulosic biomass: sugars and furfurals formation. Catalysts 2020; 10(4):437.

Wang Q, Song H, Pan S, Dong N, Wang S, Sun S. Initial pyrolysis mechanism and product formation of cellulose: an experimental and density functional theory study. Scientific Reports 2020; 10:3626.

Lim CSS, Chan EWC, Wong CW. Acetic acid as a protic solvent for reducing sulphuric acid concentrations in the production of cellulose nanocrystals alongside transition metal co-catalysts. International Journal of Biological Macromolecules 2024; 259:129303.

Toor SS, Rosendahl L, Rudolf A. Hydrothermal liquefaction of biomass: a review of subcritical water technologies. Energy 2011; 36(5):2328–2342.

Wang W, Niu M, Hou Y, Wu W, Liu Z, Liu Q, et al. Catalytic conversion of biomass-derived carbohydrates to formic acid using molecular oxygen. Green Chemistry 2014; 16(5):2614.

Kariim I, Swai H, Kivevele T. Bio-oil upgrading over ZSM-5 catalyst: a review of catalyst performance and deactivation. International Journal of Energy Research 2023.

Romañach SS, DeAngelis DL, Koh HL, Li Y, Teh SY, Barizan RSR, et al. Conservation and restoration of mangroves: global status, perspectives, and prognosis. Ocean & Coastal Management 2018; 154:72–82.

Stevenson NJ, Lewis RR, Burbridge PR. Disused shrimp ponds and mangrove rehabilitation. In: An International Perspective on Wetland Rehabilitation. Springer; 1999. p. 277–297.

Li H, Peng L, Lin L, Chen K, Zhang H. Synthesis, isolation and characterization of methyl levulinate from cellulose catalyzed by extremely low concentration acid. Journal of Energy Chemistry 2013; 22(6):895–901.

Zhang H, Lang J, Lan P, Yang H, Lu J, Wang Z. Study on the dissolution mechanism of cellulose by ChCl-based deep eutectic solvents. Materials 2020; 13(2):278.

Chen YW, Lee HV, Hamid SBA. Preparation and characterization of cellulose crystallites via Fe(III)-, Co(II)- and Ni(II)-assisted dilute sulfuric acid catalyzed hydrolysis process. Journal of Nano Research 2016; 41:96–109.

De Caprariis B, Scarsella M, Bavasso I, Bracciale MP, Tai L, De Filippis P. Effect of Ni, Zn and Fe on hydrothermal liquefaction of cellulose: impact on bio-crude yield and composition. Journal of Analytical and Applied Pyrolysis 2021; 157:105225.

Hurst G, Brangeli I, Peeters M, Tedesco S. Solid residue and by-product yields from acid-catalysed conversion of poplar wood to levulinic acid. Chemical Papers 2019; 74(5):1647–1661.

Zhou S, Yang X, Zhang Y, Jiang L, Zhou L, Lu T, et al. Efficient conversion of cellulose to methyl levulinate over heteropoly acid promoted by Sn-Beta zeolite. Cellulose 2019; 26:9135–9147.

Itabaiana Junior I, Alevar do Nascimento M, de Souza ROMA, Dufour A, Wojcieszak R. Levoglucosan: a promising platform molecule? Green Chemistry 2020; 22:5859–5880.

Jia S, Ma J, Wang D, Wang K, Zheng Q, Song C, et al. Fast and efficient upgrading of levulinic acid into long-chain alkyl levulinates fuel additives with tungsten salt catalyst at low temperature. Sustainable Energy Fuels 2020.

Ma F, Yang N, Xu C, Yu H, Wu J, Zhang X. Combination of biological pretreatment with mild acid pretreatment for enzymatic hydrolysis and ethanol production from water hyacinth. Bioresource Technology 2010; 101:9600–9604.

Son PA, Nishimura S, Ebitani K. Synthesis of levulinic acid from fructose using Amberlyst-15 as a solid acid catalyst. Reaction Kinetics, Mechanisms and Catalysis 2012; 106(1):185–192.

Yue F, Pedersen CM, Yan X, Liu Y, Xiang D, Ning C, et al. NMR studies of stock process water and reaction pathways in hydrothermal carbonization of furfural residue. Green Energy & Environment 2018; 3(2):163–171.

Zhang Y, Liu C, Chen X. Mechanism of glucose conversion in supercritical water by DFT study. Journal of Analytical and Applied Pyrolysis 2016; 119:199–207.